Received: 10 July 2018 | Revised: 14 October 2018 | Accepted: 24 October 2018

DOI: 10.1002/cne.24571

JCN RESEARCH IN SYSTEMS NEUROSCIENCE THE JOURNAL OF COMPARATIVE NEUROLOGY WILEY

REVIEW

Recent advances in mass spectrometry imaging for multiomics application in neurology

Guang Xu[1] | Jianjun Li[2]

[1]Hubei Education Cloud Service Engineering Technology Research Center, Hubei University of Education, Wuhan, China

[2]Human Health Therapeutics, National Research Council Canada, Ottawa, Ontario

Correspondence
Jianjun Li, Human Health Therapeutics, National Research Council Canada, 100 Sussex Drive, Ottawa, ON K1A 0R6.
Email: jianjun.li@nrc-cnrc.gc.ca

Funding information
Fund of Science and Technology Research Project of Hubei Provincial Department of Education, Grant/Award Number: No. B2015016

Abstract

Mass spectrometry imaging (MSI) has emerged as a powerful tool for multiomics study in neurology. MSI combines the multichannel *(m/z)* measurement capability of mass spectrometers with a surface sampling process that allows for rapid probing and mapping of the characterized intact proteins, proteolytic digested peptides, released glycans, phospholipids, glycolipids, and small metabolites in brain tissues. The present review is focused on the application of MSI to the study of proteomics, glycomics, peptidomics, metabolomics, and lipidomics in mouse brain tissues.

KEYWORDS

mass spectrometry imaging, mouse brain, proteomics, metabolomics, glycomics, lipidomics

1 | INTRODUCTION

Mass spectrometry (MS) has been widely used in the analysis of biomolecules, such as MS-based approaches for proteomics, metabolomics, lipidomics, and glycomics. It has also become evident that combine multiomics data are required to address the challenge of translational research. Mass spectrometry imaging (MSI) has emerged as a powerful tool for the direct detection of biomolecules, including proteins, peptides, glycans, metabolites, phospholipids, and glycolipids, in tissue samples (Buchberger, DeLaney, Johnson, & Li, 2018; Caprioli, 2016; Dreisewerd & Yew, 2017; Trim & Snel, 2016; Ucal et al., 2017). Several ionization sources are capable of ionizing the molecules on the surface of the sample and the mass spectrometer collects a mass spectrum at each pixel on the section with the resulting spatial resolution defined by the pixel size. The combination of data obtained from MS and visualization of spatial distributions in thin sample sections makes this a valuable chemical analysis tool for biological specimen characterization (Buchberger et al., 2018). Currently, most important ionization sources in MSI studies are matrix-assisted laser desorption/ionization (MALDI) (Caprioli, Farmer, & Gile, 1997), secondary ion mass spectrometry (SIMS) (Chandra, Smith, & Morrison, 2000), and desorption electrospray ionization (DESI) (Cooks, Ouyang, Takats, & Wiseman, 2006; Takats, Wiseman, Gologan, & Cooks, 2004). MALDI-MSI is a robust tool for spatially resolved analysis of biomolecules in situ. Because of its ability to image a wide range of molecular weights and molecular species, it allows imaging of large molecules such as proteins with spatial resolution that can reach down to the ~50 μm. (Baker, Han, & Borchers, 2017; Buchberger et al., 2018). SIMS-based MSI can be used for imaging targeted inorganic compounds (Gillen, Bennett, Tarlov, & Burgess, 1994) or biomolecules with relatively low molecular weights (Brummel, Lee, Zhou, Benkovic, & Winograd, 1994). It has the advantage of very high-spatial resolution (~100 nm), Recently, DESI technique is being increasingly used in MSI. The typical spatial resolution in DESI is ~200 μm, but this value can be reduced to 40 μm under specific operating conditions (Wu, Dill, Eberlin, Cooks, & Ifa, 2013).

Neurological disorders are diseases of the brain, spinal cord, cranial nerves, peripheral nerves, nerve roots, autonomic nervous system, neuromuscular junction, and muscles. These disorders include epilepsy, Alzheimer disease and other dementias, cerebrovascular diseases including stroke, migraine and other headache disorders, multiple sclerosis, Parkinson's disease, neuroinfections, brain tumors, traumatic disorders of the nervous system due to head trauma, and neurological disorders as a result of malnutrition (http://www.who.int/features/qa/55/en/). There is a great interest in deciphering the molecular and biochemical defects under the pathogenic process in neurological disorders. In recent years, MSI-based proteomics, glycomics, metabolomics, and lipidomics have been used as an established tool in neurological diseases. For instance, MSI-based methods can define the regions of a tissue based on their biomolecular signatures and thereby identify those regions displaying signatures associated with a brain tumor but which have not yet undergone morphological

transformation or regions that are not morphologically distinct using established histopathologic tools. Furthermore, the abundance of information available for each disease from multiple omics constitutes an advantage in identifying disease-specific underlying mechanisms. Integration of multiomics data is crucial in enhancing disease understanding and identifying meaningful clusters of molecular mechanisms in neurological disorders. This review focuses on MALDI-MSI and is designed to provide technique resource for neurologists who are interested in applying MSI for novel applications.

2 | ADVANCE IN MSI TECHNIQUES

Recent development in MALDI-MSI techniques has been greatly increasing its application in neuroscience research. The most significant development in instrumentation of MALDI-MSI includes high spatial-resolution, high mass-resolution, and coupling to ion mobility spectrometry (IMS). Attempts to use the Nd:YAG lasers for MALDI without an additional pattern generator have been made for over two decades, but were unsuccessful because of low ionization efficiency per amount of material ablated for such beam profiles at spot sizes above 50 μm (Zavalin, Yang, Haase, Holle, & Caprioli, 2014). Several strategies have been explored to increase the spatial-resolution (Anderson et al., 2014; Bauernfeind et al., 2015; Zavalin et al., 2012; Zavalin et al., 2014; Zavalin, Yang, Hayden, Vestal, & Caprioli, 2015). A Gaussian beam laser was installed in the instrument in combination with an aspheric focusing lens. This ion source produced sharp ion images at 5 μm spatial resolution with signals of high intensity as shown for images from thin tissue sections of a mouse brain (Zavalin et al., 2014). Because MALDI-MSI is often complicated by numerous high-abundance matrix derived peaks, high-mass resolution is essential to successfully implementation of MSI in the low-MW region (Amoscato et al., 2014; Verhaert, Pinkse, Strupat, & Conaway, 2010; Ye, Wang, Greer, Strupat, & Li, 2013). Thus high-resolution and high-accuracy mass spectrometers (HRMS) were used in differentiation of endogenous analytes from matrix peaks, unambiguously obtaining biomolecular distributions (Ye et al., 2013).

Coupling of IMS technologies to MS imaging allows to separate molecules according to their mobility in the gas phase after ionization, thus providing a tool to reduce the latter effect and therefore to improve the identification and image quality. This approach also allows improved detection of low abundance ions and separation of isobaric molecular species, thus resulting in more accurate determination of the spatial distribution of molecular ions (Sans, Feider, & Eberlin, 2018). IMS-MSI provides an advantage by initially separating different classes of biomolecules, such as lipids, peptides, and nucleotides, by their IM drift times prior to mass analysis (Jackson et al., 2011; Jackson et al., 2007). Traveling-wave (t-wave) ion mobility -MS (TWIMS), which uses electrodynamic rather than electrostatic fields commonly used in drift cell IM-MS instruments was developed (Ridenour, Kliman, McLean, & Caprioli, 2010), as well as application of MALDI imaging and TWIMS for separation of lipids from interfering background and peptide ions (McLean, Ridenour, & Caprioli, 2007; Ridenour et al., 2010). For example, MALDI-IMS MSI was used to investigate amyloid deposits in formalin-fixed and paraffin-embedded tissue samples. On-tissue digestion was carried out by spraying 10 layers of a trypsin solution. The results demonstrated the feasibility of IMS-MSI to investigate the amyloid's protein composition, thus paving the way to establish classification models for the diverse types of amyloidoses and to shed further light on the complex process of amyloidogenesis (Winter, Tholey, Kristen, & Rocken, 2017).

Three-dimensional (3D) MALDI-MSI is an emerging label-free bioanalytical technique capturing the spatial distribution of hundreds of molecular compounds in 3D by providing a MALDI mass spectrum for each spatial point of a 3D sample (Anderson et al., 2016; Duenas, Essner, & Lee, 2017; Giordano et al., 2016; Morosi et al., 2017; Thiele et al., 2014; Xiong et al., 2012). The first 3D MSI has used to visualize myelin basic protein in a 3D rendered volume of the corpus callosum of a mouse brain (Crecelius et al., 2005). In this study, a mouse brain was sectioned coronally at 20 μm thickness resulting in a total of 264 collected sections. Ten sections, equally spaced through the brain (400–500 μm apart), were selected for mass spectral analysis. The spatial resolution was later enhanced to 200 μm instead of 400–500 μm, thus enabling the use of virtual z-stacks and 3D volume, and to investigate differential localization patterns in much smaller brain structures, such as the substantia nigra and the interpeduncular nucleus (Andersson, Groseclose, Deutch, & Caprioli, 2008). The advent of 3D IMS has enabled a more complete picture of interactions taking place in signaling pathways and disease processes (Seeley & Caprioli, 2012).

For MALDI-MSI, the identification of matrices that cover a wider chemical scope is another factor that has been developed and optimized to improve the sensitivity of existing platforms and increase the application of MSI to even wide areas of neurological research (Cerruti, Benabdellah, Laprevote, Touboul, & Brunelle, 2012; Chan et al., 2009; Fulop et al., 2013; Ibrahim, Jurcic, Wang, Whitehead, & Yeung, 2017; Jackson et al., 2018; Liu et al., 2014; Shanta et al., 2011, 2012; Shariatgorji et al., 2012; Wang et al., 2017; Wang, Han, Yang, Pan, & Borchers, 2015; Yang & Caprioli, 2011, 2014; Zhou et al., 2017). Previously, we demonstrated that MSI technique was capable of a spatial tissue mapping of ceramide structures in gangliosides that could not be distinguished using established histologic tools (Chan et al., 2009). Silver nanoparticles were used as the matrix for MALDI-MSI to simultaneously analyze 10 classes of lipids from the brain, including fatty acids and their derivatives, sterols, CPAs, LPA and PAs, LPE and PEs, LPC and PCs, PS, Cers, SMs, and MAGs and DAGs, and other small metabolites (Guan et al., 2018). In addition, a matrix deposition procedure can also affect the MSI quality. For instance, hydration/recrystallization process was used to produce high-quality MALDI mass spectra and high-spatial-resolution ion images (Yang & Caprioli, 2011, 2014).

3 | MSI-BASED PROTEOMICS

Proteomics is the study of the function of all expressed proteins, which now encompasses not only all the proteins in any given cell, but also the set of all protein isoforms and modifications, the interactions between them, the structural description of proteins and their higher-order complexes (Tyers & Mann, 2003). Proteomics research of brain

tissues, such as a comparative proteome analysis and protein post-translational modification (PTM) characterization, will undoubtedly increase our knowledge of how proteins influence neurodegenerative diseases. Although no model can completely mimic the complexity of human diseases, animal models provide valuable contributions to biomarker discovery efforts and are important in linking biomarkers to the molecular mechanisms behind neurodegeneration (Lausted et al., 2014). By combining MSI and proteomic approaches with well-defined animal models, we do not only further our understanding of disease onset and progression, but also identify diagnostic and prognostic biomarkers that are invaluable in the development of novel therapeutic intervention strategies. In recent years, the study on localization of proteins in mouse brain tissues has been draw in a great attention, including unambiguously identification of peptides and proteins with molecular specificity, and determination of their distribution in two and three dimensions (Figure 1) (Andersson et al., 2008; Crecelius et al., 2005; Fletcher, 2015; Prentice, Ryan, Van de, Caprioli, & Spraggins, 2018; Seeley & Caprioli, 2012). Without the need for any enzymatic digestion, MSI can be used to screen for changes in expression of small proteins in brain structures implicated in the different learning phases (Aerts et al., 2017). The direct comparison of the late learning phase with the early phase revealed one protein of interest with a *m/z* of 6,724 that was detected at a considerably higher intensity in both the dorsomedial striatum (DMS) and the dorsolateral striatum (DLS). The protein also displayed higher intensities in the ventral striatum and the somatosensory and motor cortex. The authors then identified the protein as PEP-19/pcp4, which has been previously linked to cerebellar synaptic plasticity and locomotor learning. Recently, it was shown that the intact hemoglobin complex could be sampled directly from thin tissue sections of a mouse liver and correlated to a visible vascular feature, paving the way for a native MSI (Griffiths & Cooper, 2016). The method makes it possible to link the understanding of protein interactions to the protein environment by visualizing the spatial distribution of noncovalent protein interactions within tissue. The MSI study of the distribution of proteins within a mouse brain following an ischemic insult

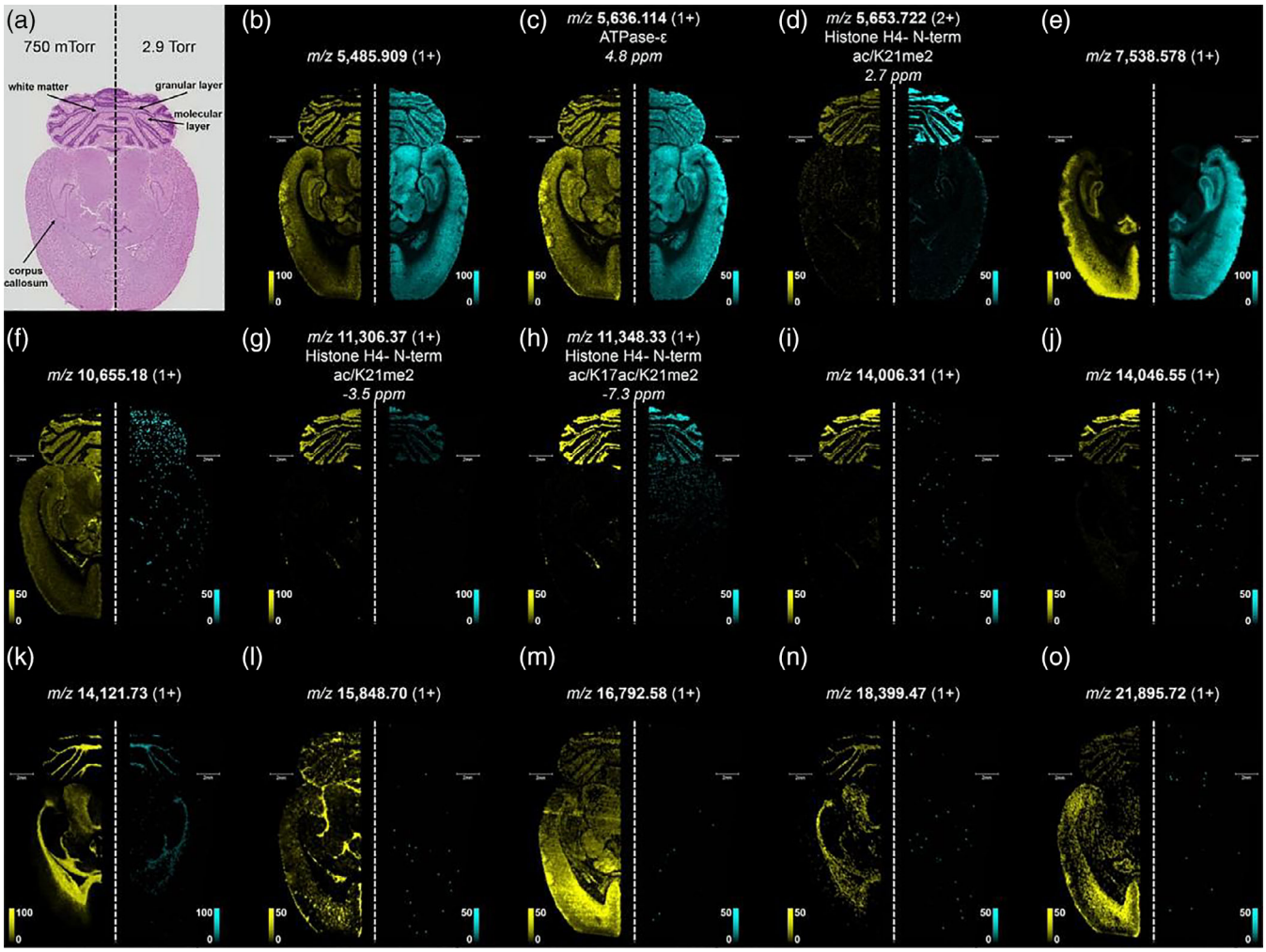

FIGURE 1 Selected ion images of intact proteins from the mass spectra displayed in Figure 5 from reference (Prentice, Ryan, Van de, Caprioli, & Spraggins, 2018). (a) An H&E stain of a serial tissue section allows for visualization of brain substructures and indicates the hemispheres of the brain that were analyzed using normal source pressure (right hemisphere) or reduced pressure source conditions (left hemisphere). (b–o) The accurate mass of the most abundant isotope and the protein charge state are reported for each of the ion images. Internal mass calibration was performed using singly and doubly charged species of cytochrome c and hemoglobin α using a quadratic fit. Images are displayed using root-mean-square (RMS) normalization. Ion images are plotted as ±0.25 Da for the most intense isotope. Scale bars = 2 mm. Reprinted with permission from Prentice, Ryan, Van de, Caprioli, and Spraggins (2018)

demonstrated that relevant proteins were involved in brain damage (Llombart et al., 2017). It revealed for the first time new proteins that might be involved in brain ischemia representing potential diagnostic biomarkers or target molecules for neurological recovery.

To increase the number of detected molecular species, two sets of sections were proposed to be collected for MSI analysis, where one set of sections could be sprayed with sinapinic acid as matrix for optimal detection of proteins and adjacent sections were applied with 2,5-dihydroxybenzoic acid (DHB) matrix for the optimal detection of low-mass species, including peptides (Andersson et al., 2008). Although the discrimination of protein expression patterns of tissues harvested from diseased and normal animals can be accomplished, it remains to be a problematic to identify proteins via MALDI-MS alone due to limited fragmentation obtained from the singly charged high-mass species, except for fairly abundant ones (Ye et al., 2014). Bottom-up MS of tryptic-digested proteins via in situ enzymatic digestion is then introduced to increase proteome coverage and to assign identities to the peaks detected by MALDI-MSI (Heijs et al., 2015; Heijs, Tolner, Bovee, van den Maagdenberg, & McDonnell, 2015). The addition of ion mobility separations into MSI workflows has allowed increased specificity and sensitivity for protein analysis, further advancing MSI into proteomics applications. Integration of MSI with TWIMS (traveling wave ion mobility spectrometry) and DTIMS (drift tube ion mobility spectrometry) has been explored for tissue analysis following on-tissue enzymatic digestions of proteins into peptides, enabling mass spectra deconvolution, as well as increased species detection, identification, and determination of their spatial distribution (Sans et al., 2018). The IMS TAG was introduced for MSI method using recombinant proteins and on-tissue digestion to detect and identify proteins from tissues using MALDI imaging and TWIMS (Cole et al., 2013). MSI of the distribution of proteins in fresh frozen and formalin-fixed paraffin-embedded tissue samples following in situ tryptic digestion were generated by isolating signals on the basis of their *m/z* value and ion mobility drift time, which were correlated to matching peptides in the recombinant standard. The tissue digestion combined with IM-TOF-IMS approach allows a proteomics "bottom-up" strategy with different types of tissue samples, especially paraffin-embedded (FFPE) tissues conserved for a long time in hospital sample banks. The combination of IM with MALDI-MSI marks the development of MSI approaches as real proteomic tools, which brings new perspectives to biological studies (Stauber et al., 2010).

MSI was also used in peptidomics, for example, determining the distribution of endogenous peptides in brain tissues (Chatterji et al., 2014; Chatterji & Pich, 2013). In the study of a rat model of Usher's disease, a rare disease considered to be a leading cause of deaf-blindness in humans worldwide, cryosections of brain tissue were analyzed to differentiate between healthy and diseased rats (Chatterji et al., 2014). Three factors were found to be important for the success of peptide quantitation. The first factor is to acquire MALDI spectra under a temperature-controlled condition. The second factor is to keep the matrix suppression below an experimentally determined limit, and the third factor is to construct the image map using the peptide-to-matrix ion abundance ratio rather than the peptide ion abundance. Recently, a method to construct a quantitatively meaningful image map from experimental data was developed (Park, Moon, Kim, Lee, & Kim, 2014). The strategy works well for contaminated tissue samples and generates quantitatively meaningful maps (Figure 2).

Amyloid beta (Abeta) deposition in the brain is an early and invariable feature of Alzheimer's disease. MSI has been used to study the spatial distribution of a broad range of Abeta species in human autopsied brains (Carlred et al., 2014, 2016; Cheng, Whitehead, Hachinski, & Cechetto, 2006; Kakuda et al., 2017; Whitehead, Cheng, Hachinski, & Cechetto, 2005; Whitehead, Hachinski, & Cechetto, 2005). Using anti-Abeta1-41 antibody, the observations from MSI and immunohistochemistry were in agreement, suggesting that a single amino acid alteration at the C-terminus of Abeta results in drastic distribution changes (Kakuda et al., 2017). For a successful MSI-based neuropeptidomic study the biological tissue sample analyzed should resemble the premortem state as much as possible (Fridjonsdottir, Nilsson, Wadensten, & Andren, 2018). Heat stabilization has been proven to inhibit postmortem degradation by denaturing proteolytic enzymes, hence increasing identification rates of neuropeptides. MSI proved to be particularly advantageous with respect to neuropeptide characterization, as commonly used antibody-based approaches target known peptide sequences and previously observed posttranslational modifications. By contrast, MALDI-MSI can unravel novel peptide processing products and thus reveal new molecular mechanisms of neuropeptide modulation of neuronal transmission (Hanrieder, Ljungdahl, & Andersson, 2012; Hanrieder, Phan, Kurczy, & Ewing, 2013). The MSI has been used to examine the integrity and distribution of the injected peptide, for example, neuropilins (NRP) inhibitory peptide (Jiang et al., 2010). In this

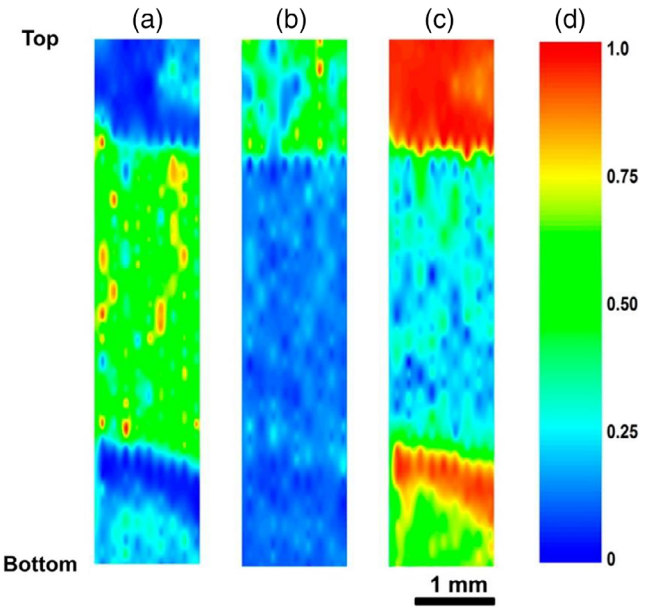

FIGURE 2 Image maps of Y5R on a tissue that was spray-coated with a solution containing CHCA and Y5R. The tissue was contaminated by larger (near the top edge) and smaller (near the bottom edge) amounts of YLYEIAR. Image maps were constructed with (a) Σili([P + H]+) and (b) Σi{Ii([P + H]+)/Ii([M + H]+)}; (c) is the suppression (equation 2) map. To draw (a), Σili([P + H]+) at each spot was normalized to the largest value in the map and color-coded according to the scale in (d); (b) was drawn similarly. To draw (c), matrix suppression at each spot was color-coded to the scale in (d). Reprinted with permission from Park, Moon, Kim, Lee, and Kim (2014)

study, MSI data revealed that NRP1 inhibitory peptide permeated a large area of the brain, both in the cortex and striatum. This approach allowed a direct visualization of the integrity and distribution of the injected NRP1 inhibitor peptide and validated the findings that neuroprotection observed in the NRP1 inhibitory peptide-treated brains was indeed due to the presence of the peptide.

4 | MSI-BASED GLYCOMICS

Protein glycosylation is one of the most important posttranslational modifications, involved in various cellular or molecular mechanisms, including protein folding and stability, molecular functional switching, signaling cascades, enzymatic activity, cancer metastasis, cell adhesion, and cell–cell interactions. A recent review highlights the multifunctional role of glycosylation in organismal diversity, involving structures, modulation, extrinsic recognition, intrinsic recognition, and molecular mimicry (Varki, 2017). The glycan and glycoprotein distributions in living organisms are rarely homogeneous. The spatial distributions of glycans in tissues and in organisms can provide fundamental understanding of the glycobiology, as well as locate specifically diseased areas (Ruhaak, Xu, Li, Goonatilleke, & Lebrilla, 2018). MALDI-MS is a highly sensitive and desired technique for screening of glycan profiles, in combination with exoglycosidase cleavage (Harvey, 2018; Ruhaak et al., 2018). Typically, N-linked glycans from eukaryotic glycoproteins are released from glycoproteins or glycopeptides using Peptide-N-Glycosidase F (PNGase F). In recent years, MSI has emerged as a novel technique for in situ analysis of N-glycome, especially in combination with PNGase F-based on-tissue digestion. It has been applied to spatially mapping of the N-glycome across formalin-fixed paraffin-embedded clinical samples (Angel, Mehta, Norris-Caneda, & Drake, 2017; Briggs et al., 2017; Drake et al., 2017; Everest-Dass et al., 2016; Heijs et al., 2016; Holst et al., 2016; Powers et al., 2013, 2014; Toghi et al., 2014). On-tissue digestion MALDI-MSI can be used to record spatially correlated molecular information from formalin-fixed, paraffin-embedded tissue sections (Everest-Dass et al., 2016; Heijs et al., 2016; Holst et al., 2016; Powers et al., 2013, 2014; Powers, Holst, Wuhrer, Mehta, & Drake, 2015; Toghi et al., 2014). It was demonstrated that no noticeable lateral diffusion was induced during the sample preparation. By combining the MSI approach with extract analysis, it was also possible to assess which mass spectral peaks generated by MALDI-MSI could be assigned to unique N-glycan and peptide identities (Heijs et al., 2016). A new approach to simultaneously map the two-dimensional distribution of N-glycans in tissues was recently reported (Powers et al., 2015). The method offered the ability to spatially profile the location and distribution of multiple N-linked glycan species released by peptide N-glycosidase F in frozen or formalin-fixed tissues. Zhang's group studied the brain sections from a C57BL/6 mouse with a resolution of 100 μm, from which forty-two N-glycans were analyzed (Figure 3) (Toghi et al., 2014). This technique consists of sectioning FFPE tissues, deparaffinization, and rehydration of the sections, denaturing of tissue proteins, release of N-linked glycans from proteins by printing peptide-N-glycosidase F over the sections, and spray-coating the tissue with matrix.

It is worth mentioning that MALDI processing is known to result in a loss of sialylation of glycan species. This limitation for the measurement of sialylated N-glycans by MALDI-MSI is confirmed by this study where the sialylated species were observed in the negative ion mode by ESI and CID fragmentation whereas MALDI-MSI in the positive ion mode had few sialylated species detected (Everest-Dass et al., 2016). To stabilize labile sialic acid residues and characterize their linkages, in situ linkage-specific derivatization was performed on FFPE tissues (Holst et al., 2016). The results showed that sialic acids were successfully stabilized in a linkage-specific manner. This strategy

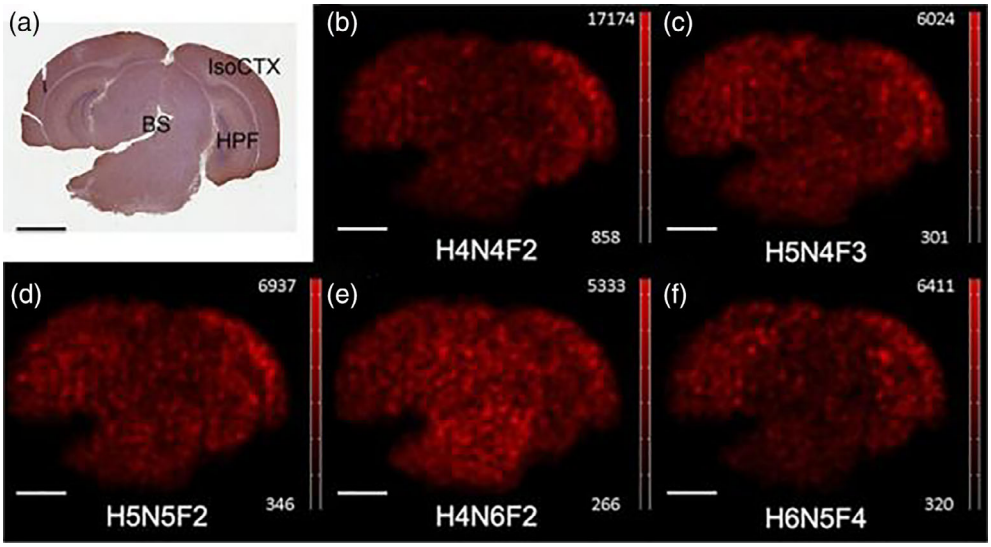

FIGURE 3 Ion images of representative fucosylated glycans along with AAL staining of an adjacent tissue section. (a) Based on the AAL histostaining, fucosylation occurs in all regions of the brain, with a relatively higher abundance in the IsoCTX compared to the HPF, while BS has the lowest abundance of fucosylation. The ion images correspond to the peaks detected at (b) 1,793.523 (H4N4F2), (c) 2,101.571 (H5N4F3), (d) 2,158.541 (H5N5F2), (e) 2,199.585 (H4N6F2), and (f) 2,613.742 (H6N5F4) Da. The signal intensity in each ion image is calculated by dividing the area of the corresponding peak by the normalized peak area of the internal glycan standard. Scale bar, 2 mm. Reproduced and slightly modified from Toghi et al. (2014) with permission

does not only increase the detection range, but also adds biological meaning to the data.

5 | MSI-BASED LIPIDOMICS

MSI has been widely used in mapping lipids in mouse brain tissues, including fatty acids (Hirahara et al., 2017; Ibrahim et al., 2017; Lerner et al., 2018; Wu, Comi, Li, Rubakhin, & Sweedler, 2016; Zhou et al., 2017), ceramides (Barbacci et al., 2017; Muller et al., 2017; Nielsen et al., 2016; Woods et al., 2013), cardiolipins (Amoscato et al., 2014; Sparvero et al., 2016), phospholipids (Angel, Spraggins, Baldwin, & Caprioli, 2012; Guo et al., 2017; Hama et al., 2018; Hankin et al., 2011; Jadoul et al., 2016; Janfelt et al., 2012; Koizumi et al., 2010; Landgraf et al., 2011; Matsumoto et al., 2011, 2017; Miyawaki et al., 2016; Shanta et al., 2011; Smith et al., 2008; Sparvero et al., 2010; Sugiura et al., 2009; Wang et al., 2017; Wang, Wang, & Han, 2018; Whitehead et al., 2007; Zaima et al., 2014), and sphingolipids (Caughlin et al., 2015, 2017; Caughlin, Park, Yeung, Cechetto, & Whitehead, 2017; Chan et al., 2009; Dufresne et al., 2017; Ermini et al., 2017; Goto-Inoue et al., 2010; Jackson et al., 2011, 2018; Jones et al., 2017; Meriaux, Franck, Wisztorski, Salzet, & Fournier, 2010; Sugiura, Shimma, Konishi, Yamada, & Setou, 2008; Weishaupt, Caughlin, Yeung, & Whitehead, 2015; Whitehead et al., 2011). Gangliosides, amphipathic molecules composed of a ceramide lipid anchor linked to an oligosaccharide, are sialic acid-containing glycosphingolipids and play numerous important roles in neuronal functions. Unfortunately, MALDI imparts higher energy during ionization causing an instability of analyte ions and sometimes inducing unwanted fragmentation. This is a major hurdle for imaging gangliosides in tissue, as sialic acid residues can be dissociated in ionization process. To minimize the loss of sialic acid during ionization processing, we investigated an ionic liquid matrix for MSI of gangliosides (Chan et al., 2009). This ionic liquid matrix offered excellent sensitivity for detection of gangliosides without significant loss of sialic acid residues, which was used to study the abundance and anatomical localization of gangliosides in a mouse brain using MSI technique. The MSI analyses of the mouse brain tissue sections demonstrated that the N-fatty acyl chains of gangliosides were differentially distributed in hippocampal regions, whereby the gangliosides with N-C18 acyl chain were enriched in CA1 region, while gangliosides with N-C20 acyl chain were enriched in dentate gyrus (Figure 4). In addition, this observation is the same for mono-, di-, and tri-sialylated gangliosides. MSI is also applicable to examine the neuroanatomical distribution of A-series gangliosides with either 18 or 20 carbon sphingosine chains (d18:1 or d20:1) in rats across the lifespan. The ratio of d20:1/d18:1 species was determined across 11 regions of interest in the brain. Interestingly, a decrease in the d20:1/d18:1 ratio for GM2 and GM3 was observed during early development with the exception of the periventricular corpus callosum, whereas an age-dependent increase was observed for GM3 (Caughlin, Maheshwari, et al., 2017). Several other ionic matrixes based on 2,5-dihydroxybenzoic acid were synthesized and tested for lipid analysis on tissues, including 2,5-DHB/ANI, 2,5-DHB/DANI, 2,5-DHB/DEANI, 2,5-DHB/Pyr, and 2,5-DHB/3-AP, where ANI, DANI, DEANI, Pyr, 3-AP stand for aniline, N,N-dimethylaniline, N,N-diethylaniline, pyridine, and 3-acetylpyridine, respectively (Meriaux et al., 2010).

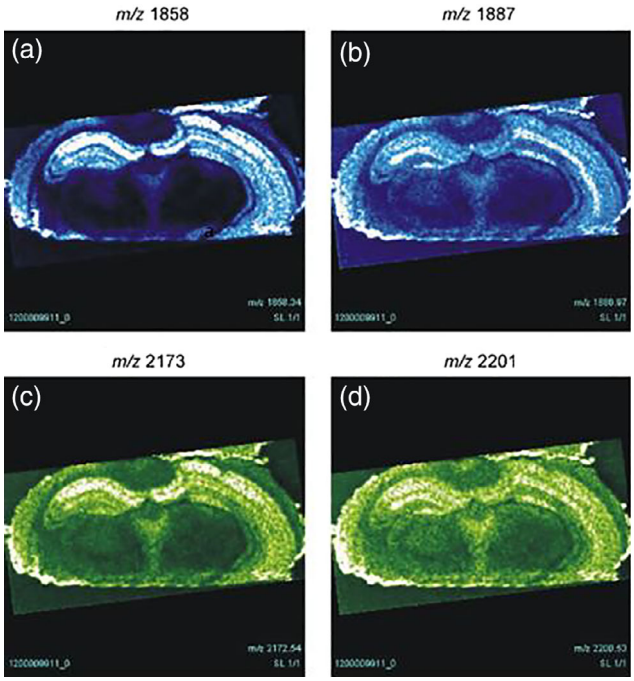

FIGURE 4 Negative ion mode imaging of mouse brain analyzed with MALDI-TOF. (a) GDx distribution at m/z 1858 (C18:1/C18:0); (b) GDx distribution at *m/z* 1887 (C18:1/C20:0); (c) GTx distribution at *m/z* 2,173 (C18:1/C18:0); and (d) GTx distribution at *m/z* 2,173 (C18:1/C20:0). Reproduced and slightly modified from Chan et al. (2009) with permission

MSI technique was used to examine the spatial profile of ganglioside species following middle cerebral artery occlusion (MCAO)-reperfusion injury in the mouse (Whitehead et al., 2011; Whitehead, Gangaraju, Slinn, & Hou, 2010). Significant differences in the ratio of expression between ipsilateral and contralateral cortices were found for various detected ganglioside species following MCAO-reperfusion injury. The results revealed that brain region specific expression of gangliosides, particularly with respect to the hydrocarbon length, may play a role in neuronal responses to injury. Fourier transform infrared (FTIR) microscopy and MSI were integrated for analysis of single-slide tissue specimen (Rabe et al., 2018). FTIR microscopy can automatically guide high-resolution MSI data acquisition and interpretation without requiring prior histopathological tissue annotation, thus circumventing potential human-annotation-bias, while achieving >90% reductions of data load and acquisition time. The general applicability of multimodal FTIR-guided MSI was demonstrated with a precise tumor localization in a mouse brain bearing glioma xenografts and in human primary gastrointestinal stromal tumors. This multimodal tissue analysis method allows for morphology-sensitive lipid signature retrieval from brains of mice suffering from lipidosis caused by Niemann-Pick type C disease.

Mild traumatic brain injury (TBI) is a common public health issue that may contribute to chronic degenerative disorders. Membrane lipids play a key role in tissue responses to injury, both as cell signals and as components of membrane structure and cell signaling. MSI has

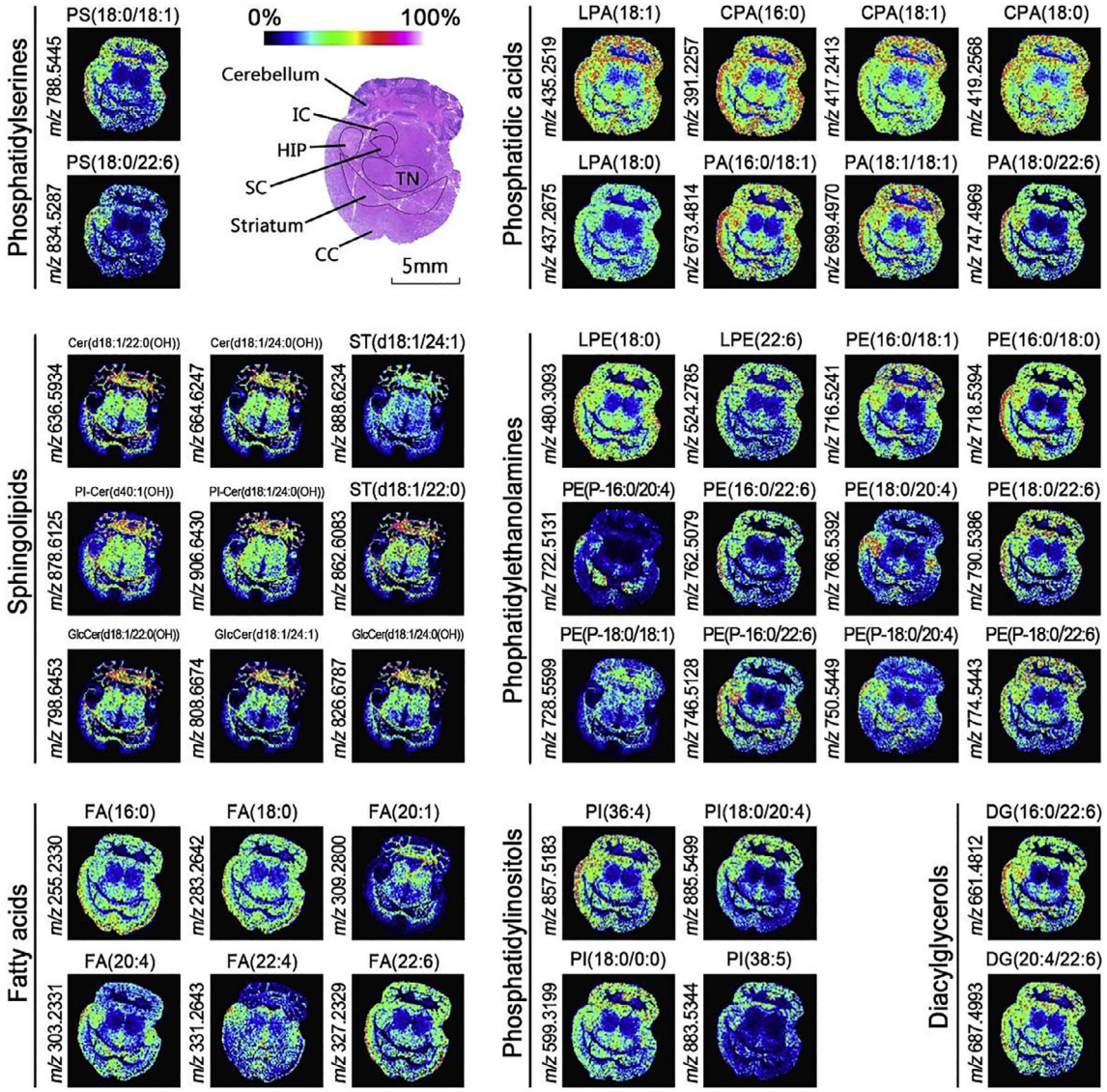

FIGURE 5 Optical image of H&E stained mouse brain horizontal tissue section and the ion images of different lipid classes. MSI data were acquired with a spatial resolution of 200 μm. HIP = Hippocampus; SC = superior colliculus; IC = inferior colliculus; TN = thalamic nucleus; CC = cerebral cortex. Reprinted with permission from Zhou, Guo et al. (2017)

been used to assess sequences of responses of lipid species in a rat controlled cortical impact model for concussion (Roux et al., 2016). In combination with in vivo PET imaging, MSI was used to investigate different aspects of stroke recovery (Henderson et al., 2018). Three months after stroke, PET imaging showed minimal detection of neurodegeneration and neuroinflammation, indicating that the brain has stabilized. However, MSI revealed distinct differences in lipid distributions, (e.g., phosphatidylcholine and sphingomyelin) between the scar and the healthy brain, suggesting that recovery processes were still in play. With histology and microscopy used for identification of anatomical landmarks, MSI and LC–MS were used to characterize the lipidome of the subventricular zone (Hunter, Demarais, Faull, Grey, & Curtis, 2018). It was found that the subventricular zone was rich in sphingomyelins and phosphatidylserines but deficient in phosphatidylethanolamines. The ependymal layer had an abundance of phosphatidylinositols, whereas the myelin layer was rich in sulfatides and triglycerides. The hypocellular layer showed enrichment of sphingomyelins. No discrete lipid signature was seen in the astrocytic ribbon. MSI analysis of a mouse brain revealed the distribution of 44:1 PtdCho (phosphatidylcholine), which contains 26:0 FA in the brain (Hama et al., 2018). This is the first report describing the spatial dissection of phospholipid species with very long-chain fatty acid(s) in the brain by MSI. It has been reported that cardiolipin (CL) is selectively oxidized and presents itself as a target for the redox therapy following TBI. However, the topography of changes of CL in the injured brain remained to be defined. CL is a mitochondria-specific structurally unusual anionic phospholipid containing four fatty acyl chains. MSI of a controlled cortical impact model of TBI in rats revealed that TBI caused early decreases in CL in the contusional cortex, ipsilateral hippocampus, and thalamus with the most highly unsaturated CL species being most susceptible to loss. Phosphatidylinositol was the only other lipid species that exhibited a significant decrease, albeit to a lesser extent than CL. Signals for other lipids remained unchanged (Sparvero et al., 2016).

6 | MSI-BASED METABOLOMICS

Mass spectrometry is a major analysis platform used in metabolomics, providing wide metabolite coverage. Because of its high sensitivity and selectivity, MSI is useful for the investigation of exogenous and endogenous compounds, including intermediates and end products of metabolic pathways. MSI of neurotransmitters has so far been mainly performed using MALDI as ion source, where derivatization reagents, deuterated matrix and/or high resolution, or tandem MS have been applied to circumvent problems with interfering ion peaks from matrix and from isobaric species (Fernandes et al., 2016). However, MALDI-MSI of metabolites and neurotransmitters present at physiological concentrations in tissues is often complicated by numerous high-abundance matrix-derived peaks (Trim & Snel, 2016). High selectivity is therefore essential to successfully implement MSI in the low-MW region (Ye et al., 2013). However, small molecule analysis is still far from being fully reached due to the limited sensitivity and matrix interference. Thus, graphene oxide (GO) was proposed as a MALDI matrix to image small molecules in tissues in negative ion mode (Figure 5). MALDI imaging of small molecules in mouse brain tissue sections coated with the GO matrix was performed by Fourier transform ion cyclotron resonance mass spectrometry (FTICR MS) in negative ion mode.

Analysis of the distribution of small synthetic drugs and their metabolites is important in the development of new treatment approaches. Linking biology through histology and the intrinsic chemical properties of drugs and their metabolites could be translational in drug development (Castellino, Groseclose, & Wagner, 2011). MSI has also demonstrated its applicability in search of alternative animal models such as zebrafish, *Danio rerio*, and the desert locust, *Schistocerca gregaria*, which can be efficiently used in early drug discovery to evaluate the drug activity and pharmacokinetic properties of potential drugs and toxins in the central nervous system, (Villacrez et al., 2018). Recently, several of on-tissue chemical derivatization strategies have been independently reported that enable the detection of amino neurotransmitters (Esteve, Jones, Kell, Boutin, & McDonnell, 2017; Esteve, Tolner, Shyti, van den Maagdenberg, & McDonnell, 2016). This study demonstrated the visualization of the distribution of up to 23 amino metabolites in tissue (Figure 6). The methodology was further used to detect alterations of these compounds, following the

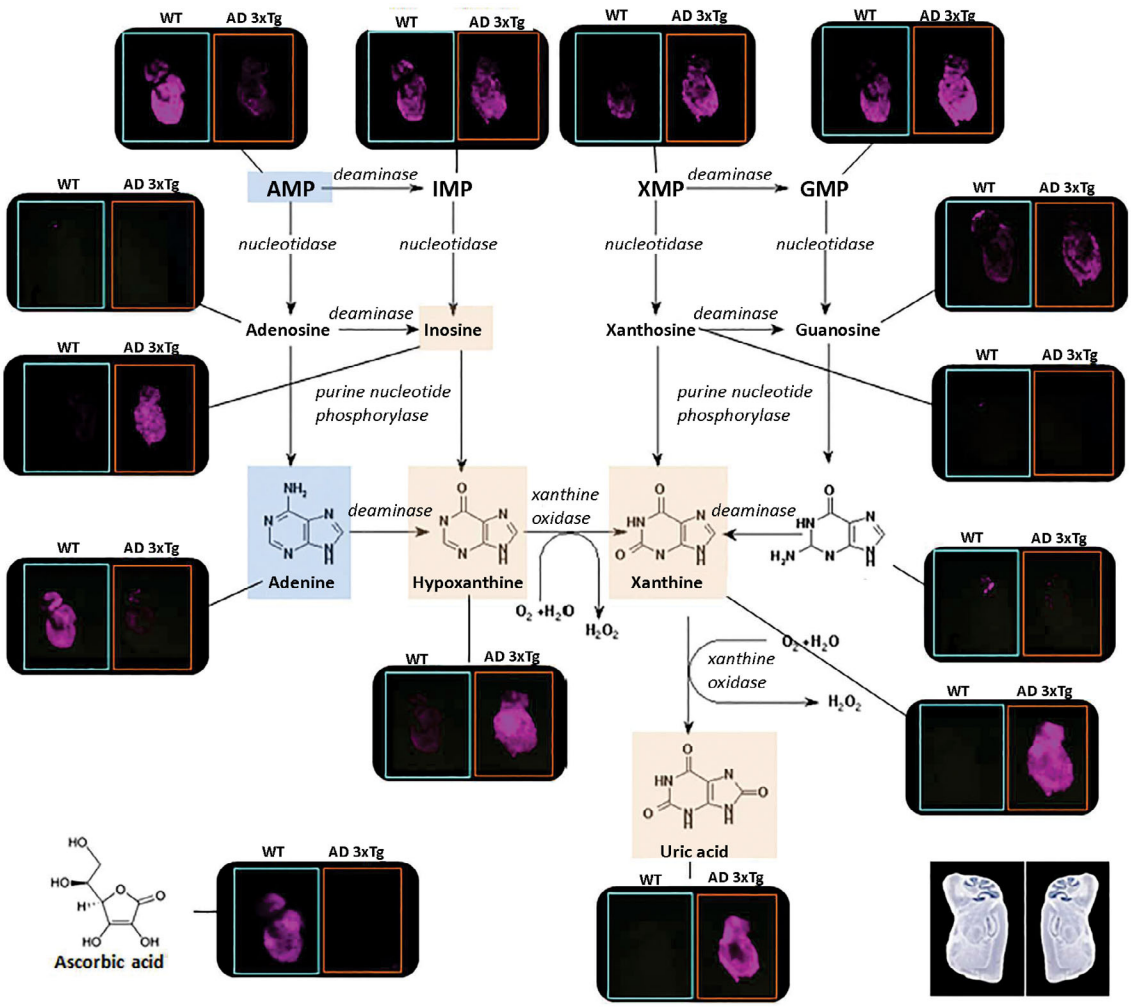

FIGURE 6 MALDI-FTICR-MSI visualization of accurate mass (<1 ppm) and isotope profile filtered (Pearson correlation >0.95) metabolites involved the purine metabolic pathway for WT and 3 × Tg mice. All tissue sections are sagittal with the cerebellum located at the top. Scale bar = 2 mm. Reprinted with permission from Esteve, Jones, Kell, Boutin, and McDonnell (2017)

introduction of an experimental cortical spreading depression in a mouse brain, which cause profound transient alterations in key neurotransmitters in one hemisphere and could be relevant to migraine and various other neurological disorders (Esteve et al., 2016). An interesting shift toward proinflammatory molecules (uric acid) in the purinergic pathway was observed, which associated with a decrease in antioxidant level (ascorbic acid). Together, these observations fit well with the increased oxidative stress and neuroinflammation commonly observed in AD (Esteve, Jones et al., 2017). The ability of MALDI imaging to provide a greater understanding of drug and metabolite tissue distribution is very exciting and at the heart of the widespread interest in this technique.

7 | CONCLUSION

MSI has become an important tool to study multiomics in neurology. It is capable of providing localization information on proteins, glycans, metabolites, and lipids in tissues. In recent years, significant efforts have been made to structurally or quantitatively characterize the multiomics of brain samples from a variety of animal models. MSI has been used to investigate the altered biological molecule profiles and their distributions in a wide assortment of diseases. It is worthy to point out that the technological development in MSI, including higher mass resolution and higher detection sensitivity, will certainly play a crucial role in advancing the application of MSI in neurology. New sample preparation strategies, including new matrix materials and novel matrix deposition methods, will be highly desirable to improve the quality of MSI data.

ACKNOWLEDGMENTS

This work was supported by grant from the Fund of Science and Technology Research Project of Hubei Provincial Department of Education (No. B2015016) to G.X.

ORCID

Guang Xu https://orcid.org/0000-0002-8775-1987

REFERENCES

Aerts, J., Laeremans, A., Minerva, L., Boonen, K., Harshavardhan, B., D'hooge, R., … Arckens, L. (2017). MS imaging and mass spectrometric synaptosome profiling identify PEP-19/pcp4 as a synaptic molecule involved in spatial learning in mice. *Biochimica et Biophysica Acta*, *1865*, 936–945.

Amoscato, A. A., Sparvero, L. J., He, R. R., Watkins, S., Bayir, H., & Kagan, V. E. (2014). Imaging mass spectrometry of diversified cardiolipin molecular species in the brain. *Analytical Chemistry*, *86*, 6587–6595.

Anderson, D. M., Ablonczy, Z., Koutalos, Y., Spraggins, J., Crouch, R. K., Caprioli, R. M., & Schey, K. L. (2014). High resolution MALDI imaging mass spectrometry of retinal tissue lipids. *Journal of the American Society for Mass Spectrometry*, *25*, 1394–1403.

Anderson, D. M., Van de, P. R., Rose, K. L., Hill, S., Schey, K. L., Solga, A. C., … Caprioli, R. M. (2016). 3-D imaging mass spectrometry of protein distributions in mouse Neurofibromatosis 1 (NF1)-associated optic glioma. *Journal of Proteomics*, *149*, 77–84.

Andersson, M., Groseclose, M. R., Deutch, A. Y., & Caprioli, R. M. (2008). Imaging mass spectrometry of proteins and peptides: 3D volume reconstruction. *Nature Methods*, *5*, 101–108.

Angel, P. M., Mehta, A., Norris-Caneda, K., & Drake, R. R. (2017). MALDI imaging mass spectrometry of N-glycans and Tryptic peptides from the same formalin-fixed, paraffin-embedded tissue section. *Methods in Molecular Biology*, *1788*, 225–241.

Angel, P. M., Spraggins, J. M., Baldwin, H. S., & Caprioli, R. (2012). Enhanced sensitivity for high spatial resolution lipid analysis by negative ion mode matrix assisted laser desorption ionization imaging mass spectrometry. *Analytical Chemistry*, *84*, 1557–1564.

Baker, T. C., Han, J., & Borchers, C. H. (2017). Recent advancements in matrix-assisted laser desorption/ionization mass spectrometry imaging. *Current Opinion in Biotechnology*, *43*, 62–69.

Barbacci, D. C., Roux, A., Muller, L., Jackson, S. N., Post, J., Baldwin, K., … Woods, A. S. (2017). Mass spectrometric imaging of Ceramide biomarkers tracks therapeutic response in traumatic brain injury. *ACS Chemical Neuroscience*, *8*, 2266–2274.

Bauernfeind, A. L., Reyzer, M. L., Caprioli, R. M., Ely, J. J., Babbitt, C. C., Wray, G. A., … Sherwood, C. C. (2015). High spatial resolution proteomic comparison of the brain in humans and chimpanzees. *The Journal of Comparative Neurology*, *523*, 2043–2061.

Briggs, M. T., Ho, Y. Y., Kaur, G., Oehler, M. K., Everest-Dass, A. V., Packer, N. H., & Hoffmann, P. (2017). N-glycan matrix-assisted laser desorption/ionization mass spectrometry imaging protocol for formalin-fixed paraffin-embedded tissues. *Rapid Communications in Mass Spectrometry*, *31*, 825–841.

Brummel, C. L., Lee, I. N., Zhou, Y., Benkovic, S. J., & Winograd, N. (1994). A mass spectrometric solution to the address problem of combinatorial libraries. *Science*, *264*(5157), 399–402.

Buchberger, A. R., DeLaney, K., Johnson, J., & Li, L. (2018). Mass spectrometry imaging: A review of emerging advancements and future insights. *Analytical Chemistry*, *90*, 240–265.

Caprioli, R. M. (2016). Imaging mass spectrometry: Molecular microscopy for the new age of biology and medicine. *Proteomics*, *16*, 1607–1612.

Caprioli, R. M., Farmer, T. B., & Gile, J. (1997). Molecular imaging of biological samples: Localization of peptides and proteins using MALDI-TOF MS. *Analytical Chemistry*, *69*, 4751–4760.

Carlred, L., Gunnarsson, A., Sole-Domenech, S., Johansson, B., Vukojevic, V., Terenius, L., … Sjovall, P. (2014). Simultaneous imaging of amyloid-beta and lipids in brain tissue using antibody-coupled liposomes and time-of-flight secondary ion mass spectrometry. *Journal of the American Chemical Society*, *136*, 9973–9981.

Carlred, L., Michno, W., Kaya, I., Sjovall, P., Syvanen, S., & Hanrieder, J. (2016). Probing amyloid-beta pathology in transgenic Alzheimer's disease (tgArcSwe) mice using MALDI imaging mass spectrometry. *Journal of Neurochemistry*, *138*, 469–478.

Castellino, S., Groseclose, M. R., & Wagner, D. (2011). MALDI imaging mass spectrometry: Bridging biology and chemistry in drug development. *Bioanalysis*, *3*, 2427–2441.

Caughlin, S., Hepburn, J. D., Park, D. H., Jurcic, K., Yeung, K. K., Cechetto, D. F., & Whitehead, S. N. (2015). Increased expression of simple Ganglioside species GM2 and GM3 detected by MALDI imaging mass spectrometry in a combined rat model of Abeta toxicity and stroke. *PLoS One*, *10*, e0130364.

Caughlin, S., Maheshwari, S., Weishaupt, N., Yeung, K. K., Cechetto, D. F., & Whitehead, S. N. (2017). Age-dependent and regional heterogeneity in the long-chain base of A-series gangliosides observed in the rat brain using MALDI imaging. *Scientific Reports*, *7*, 16135.

Caughlin, S., Park, D. H., Yeung, K. K., Cechetto, D. F., & Whitehead, S. N. (2017). Sublimation of DAN matrix for the detection and visualization of Gangliosides in rat brain tissue for MALDI imaging mass spectrometry. *Journal of Visualized Experiments*, *121*, e55254-1–e55254-8.

Cerruti, C. D., Benabdellah, F., Laprevote, O., Touboul, D., & Brunelle, A. (2012). MALDI imaging and structural analysis of rat brain lipid negative ions with 9-aminoacridine matrix. *Analytical Chemistry*, *84*, 2164–2171.

Chan, K., Lanthier, P., Liu, X., Sandhu, J. K., Stanimirovic, D., & Li, J. (2009). MALDI mass spectrometry imaging of gangliosides in mouse brain using ionic liquid matrix. *Analytica Chimica Acta*, *639*, 57–61.

Chandra, S., Smith, D. R., & Morrison, G. H. (2000). Subcellular imaging by dynamic SIMS ion microscopy. *Analytical Chemistry*, *72*, 104A–114A.

Chatterji, B., Dickhut, C., Mielke, S., Kruger, J., Just, I., Glage, S., … Pich, A. (2014). MALDI imaging mass spectrometry to investigate endogenous peptides in an animal model of Usher's disease. *Proteomics*, *14*, 1674–1687.

Chatterji, B., & Pich, A. (2013). MALDI imaging mass spectrometry and analysis of endogenous peptides. *Expert Review of Proteomics*, *10*, 381–388.

Cheng, G., Whitehead, S. N., Hachinski, V., & Cechetto, D. F. (2006). Effects of pyrrolidine dithiocarbamate on beta-amyloid (25-35)-induced inflammatory responses and memory deficits in the rat. *Neurobiology of Disease*, *23*, 140–151.

Cole, L. M., Mahmoud, K., Haywood-Small, S., Tozer, G. M., Smith, D. P., & Clench, M. R. (2013). Recombinant "IMS TAG" proteins--a new method for validating bottom-up matrix-assisted laser desorption/ionisation ion mobility separation mass spectrometry imaging. *Rapid Communications in Mass Spectrometry*, *27*, 2355–2362.

Cooks, R. G., Ouyang, Z., Takats, Z., & Wiseman, J. M. (2006). Detection technologies ambient mass spectrometry. *Science*, *311*, 1566–1570.

Crecelius, A. C., Cornett, D. S., Caprioli, R. M., Williams, B., Dawant, B. M., & Bodenheimer, B. (2005). Three-dimensional visualization of protein expression in mouse brain structures using imaging mass spectrometry. *Journal of the American Society for Mass Spectrometry*, *16*, 1093–1099.

Drake, R. R., Powers, T. W., Jones, E. E., Bruner, E., Mehta, A. S., & Angel, P. M. (2017). MALDI mass spectrometry imaging of N-linked Glycans in cancer tissues. *Advances in Cancer Research*, *134*, 85–116.

Dreisewerd, K., & Yew, J. Y. (2017). Mass spectrometry imaging goes three dimensional. *Nature Methods*, *14*, 1139–1140.

Duenas, M. E., Essner, J. J., & Lee, Y. J. (2017). 3D MALDI mass spectrometry imaging of a single cell: Spatial mapping of lipids in the embryonic development of Zebrafish. *Scientific Reports*, *7*, 14946.

Dufresne, M., Guneysu, D., Patterson, N. H., Marcinkiewicz, M. M., Regina, A., Demeule, M., & Chaurand, P. (2017). Multimodal detection of GM2 and GM3 lipid species in the brain of mucopolysaccharidosis type II mouse by serial imaging mass spectrometry and immunohistochemistry. *Analytical and Bioanalytical Chemistry*, *409*, 1425–1433.

Ermini, L., Morganti, E., Post, A., Yeganeh, B., Caniggia, I., Leadley, M., … Post, M. (2017). Imaging mass spectrometry identifies prognostic ganglioside species in rodent intracranial transplants of glioma and medulloblastoma. *PLoS One*, *12*, e0176254.

Esteve, C., Jones, E. A., Kell, D. B., Boutin, H., & McDonnell, L. A. (2017). Mass spectrometry imaging shows major derangements in neurogranin and in purine metabolism in the triple-knockout 3xTg Alzheimer mouse model. *Biochimica et Biophysica Acta*, *1865*, 747–754.

Esteve, C., Tolner, E. A., Shyti, R., van den Maagdenberg, A. M., & McDonnell, L. A. (2016). Mass spectrometry imaging of amino neurotransmitters: A comparison of derivatization methods and application in mouse brain tissue. *Metabolomics*, *12*, 30.

Everest-Dass, A. V., Briggs, M. T., Kaur, G., Oehler, M. K., Hoffmann, P., & Packer, N. H. (2016). N-glycan MALDI imaging mass spectrometry on formalin-fixed paraffin-embedded tissue enables the delineation of ovarian cancer tissues. *Molecular & Cellular Proteomics*, *15*, 3003–3016.

Fernandes, A. M., Vendramini, P. H., Galaverna, R., Schwab, N. V., Alberici, L. C., Augusti, R., … Eberlin, M. N. (2016). Direct visualization of neurotransmitters in rat brain slices by desorption electrospray ionization mass spectrometry imaging (D). *Journal of the American Society for Mass Spectrometry*, *27*, 1944–1951.

Fletcher, J. S. (2015). 3D imaging of biological specimen using MS. *Bioanalysis*, *7*, 2657–2666.

Fridjonsdottir, E., Nilsson, A., Wadensten, H., & Andren, P. E. (2018). Brain tissue sample stabilization and extraction strategies for Neuropeptidomics. *Methods in Molecular Biology*, *1719*, 41–49.

Fulop, A., Porada, M. B., Marsching, C., Blott, H., Meyer, B., Tambe, S., … Hopf, C. (2013). 4-phenyl-alpha-cyanocinnamic acid amide: Screening for a negative ion matrix for MALDI-MS imaging of multiple lipid classes. *Analytical Chemistry*, *85*, 9156–9163.

Gillen, G., Bennett, J., Tarlov, M. J., & Burgess, D. R. F. (1994). Molecular imaging secondary ion mass spectrometry for the characterization of patterned self-assembled monolayers on silver and gold. *Analytical Chemistry*, *66*(13), 2170–2174.

Giordano, S., Morosi, L., Veglianese, P., Licandro, S. A., Frapolli, R., Zucchetti, M., … Davoli, E. (2016). 3D mass spectrometry imaging reveals a very heterogeneous drug distribution in tumors. *Scientific Reports*, *6*, 37027.

Goto-Inoue, N., Hayasaka, T., Zaima, N., Kashiwagi, Y., Yamamoto, M., Nakamoto, M., & Setou, M. (2010). The detection of glycosphingolipids in brain tissue sections by imaging mass spectrometry using gold nanoparticles. *Journal of the American Society for Mass Spectrometry*, *21*, 1940–1943.

Griffiths, R. L., & Cooper, H. J. (2016). Direct tissue profiling of protein complexes: Toward native mass spectrometry imaging. *Analytical Chemistry*, *88*, 606–609.

Guan, M., Zhang, Z., Li, S., Liu, J., Liu, L., Yang, H., … Zhao, Z. (2018). Silver nanoparticles as matrix for MALDI FTICR MS profiling and imaging of diverse lipids in brain. *Talanta*, *179*, 624–631.

Guo, S., Zhou, D., Zhang, M., Li, T., Liu, Y., Xu, Y., … Li, Z. (2017). Monitoring changes of docosahexaenoic acid-containing lipids during the recovery process of traumatic brain injury in rat using mass spectrometry imaging. *Scientific Reports*, *7*, 5054.

Hama, K., Fujiwara, Y., Morita, M., Yamazaki, F., Nakashima, Y., Takei, S., … Yokoyama, K. (2018). Profiling and imaging of phospholipids in brains of Abcd1-deficient mice. *Lipids*, *53*, 85–102.

Hankin, J. A., Farias, S. E., Barkley, R. M., Heidenreich, K., Frey, L. C., Hamazaki, K., … Murphy, R. C. (2011). MALDI mass spectrometric imaging of lipids in rat brain injury models. *Journal of the American Society for Mass Spectrometry*, *22*, 1014–1021.

Hanrieder, J., Ljungdahl, A., & Andersson, M. (2012). MALDI imaging mass spectrometry of neuropeptides in Parkinson's disease. *Journal of Visualized Experiments*, *60*, e3445-1–e3445-5.

Hanrieder, J., Phan, N. T., Kurczy, M. E., & Ewing, A. G. (2013). Imaging mass spectrometry in neuroscience. *ACS Chemical Neuroscience*, *4*, 666–679.

Harvey, D. J. (2018). Analysis of carbohydrates and glycoconjugates by matrix-assisted laser desorption/ionization mass spectrometry: An update for 2013-2014. *Mass Spectrometry Reviews*, *37*, 353–491.

Heijs, B., Carreira, R. J., Tolner, E. A., de Ru, A. H., van den Maagdenberg, A. M., van Veelen, P. A., & McDonnell, L. A. (2015). Comprehensive analysis of the mouse brain proteome sampled in mass spectrometry imaging. *Analytical Chemistry*, *87*, 1867–1875.

Heijs B, Holst S, Briaire-de B, I, van Pelt GW, de Ru AH, van Veelen PA, Drake RR, Mehta AS, Mesker WE, Tollenaar RA, Bovee JV, Wuhrer M, McDonnell LA. Multimodal mass spectrometry imaging of N-Glycans and proteins from the same tissue section. *Analytical Chemistry*, 2016; *88*: 7745–53.

Heijs, B., Tolner, E. A., Bovee, J. V., van den Maagdenberg, A. M., & McDonnell, L. A. (2015). Brain region-specific dynamics of on-tissue protein digestion using MALDI mass spectrometry imaging. *Journal of Proteome Research*, *14*, 5348–5354.

Henderson, F., Hart, P. J., Pradillo, J. M., Kassiou, M., Christie, L., Williams, K. J., … McMahon, A. (2018). Multi-modal imaging of long term recovery post-stroke by PET and MALDI-MS. *Rapid Communications in Mass Spectrometry*, *32*, 721–729.

Hirahara, Y., Wakabayashi, T., Mori, T., Koike, T., Yao, I., Tsuda, M., … Yamada, H. (2017). Sulfatide species with various fatty acid chains in oligodendrocytes at different developmental stages determined by imaging mass spectrometry. *Journal of Neurochemistry*, *140*, 435–450.

Holst, S., Heijs, B., de, H. N., van Zeijl, R. J., Briaire-de, B. I., van Pelt, G. W., … Wuhrer, M. (2016). Linkage-specific in situ Sialic acid Derivatization for N-glycan mass spectrometry imaging of formalin-fixed paraffin-embedded tissues. *Analytical Chemistry*, *88*, 5904–5913.

Hunter, M., Demarais, N. J., Faull, R. L. M., Grey, A. C., & Curtis, M. A. (2018). Layer-specific lipid signatures in the human subventricular zone demonstrated by imaging mass spectrometry. *Scientific Reports*, *8*, 2551.

Ibrahim, H., Jurcic, K., Wang, J. S., Whitehead, S. N., & Yeung, K. K. (2017). 1,6-Diphenyl-1,3,5-hexatriene (DPH) as a novel matrix for MALDI MS imaging of fatty acids, phospholipids, and Sulfatides in brain tissues. *Analytical Chemistry*, *89*, 12828–12836.

Jackson, S. N., Colsch, B., Egan, T., Lewis, E. K., Schultz, J. A., & Woods, A. S. (2011). Gangliosides' analysis by MALDI-ion mobility MS. *Analyst*, *136*, 463–466.

Jackson, S. N., Muller, L., Roux, A., Oktem, B., Moskovets, E., Doroshenko, V. M., & Woods, A. S. (2018). AP-MALDI mass spectrometry imaging

of Gangliosides using 2,6-Dihydroxyacetophenone. *Journal of the American Society for Mass Spectrometry*, *29*, 1463–1472.

Jackson, S. N., Ugarov, M., Egan, T., Post, J. D., Langlais, D., Albert, S. J., & Woods, A. S. (2007). MALDI-ion mobility-TOFMS imaging of lipids in rat brain tissue. *Journal of Mass Spectrometry*, *42*, 1093–1098.

Jadoul, L., Smargiasso, N., Pamelard, F., Alberts, D., Noel, A., De, P. E., & Longuespee, R. (2016). An improved molecular histology method for ion suppression monitoring and quantification of Phosphatidyl Cholines during MALDI MSI Lipidomics analyses. *OMICS*, *20*, 110–121.

Janfelt, C., Wellner, N., Leger, P. L., Kokesch-Himmelreich, J., Hansen, S. H., Charriaut-Marlangue, C., & Hansen, H. S. (2012). Visualization by mass spectrometry of 2-dimensional changes in rat brain lipids, including N-acylphosphatidylethanolamines, during neonatal brain ischemia. *The FASEB Journal*, *26*, 2667–2673.

Jiang, S. X., Whitehead, S., Aylsworth, A., Slinn, J., Zurakowski, B., Chan, K., … Hou, S. T. (2010). Neuropilin 1 directly interacts with Fer kinase to mediate semaphorin 3A-induced death of cortical neurons. *The Journal of Biological Chemistry*, *285*, 9908–9918.

Jones, E. E., Zhang, W., Zhao, X., Quiason, C., Dale, S., Shahidi-Latham, S., … Sun, Y. (2017). Tissue localization of Glycosphingolipid accumulation in a Gaucher disease mouse brain by LC-ESI-MS/MS and high-resolution MALDI imaging mass spectrometry. *SLAS. Discov.*, *22*, 1218–1228.

Kakuda, N., Miyasaka, T., Iwasaki, N., Nirasawa, T., Wada-Kakuda, S., Takahashi-Fujigasaki, J., … Ikegawa, M. (2017). Distinct deposition of amyloid-beta species in brains with Alzheimer's disease pathology visualized with MALDI imaging mass spectrometry. *Acta Neuropathologica Communications*, *5*, 73.

Koizumi, S., Yamamoto, S., Hayasaka, T., Konishi, Y., Yamaguchi-Okada, M., Goto-Inoue, N., … Namba, H. (2010). Imaging mass spectrometry revealed the production of lyso-phosphatidylcholine in the injured ischemic rat brain. *Neuroscience*, *168*, 219–225.

Landgraf, R. R., Garrett, T. J., Conaway, M. C., Calcutt, N. A., Stacpoole, P. W., & Yost, R. A. (2011). Considerations for quantification of lipids in nerve tissue using matrix-assisted laser desorption/ionization mass spectrometric imaging. *Rapid Communications in Mass Spectrometry*, *25*, 3178–3184.

Lausted, C., Lee, I., Zhou, Y., Qin, S., Sung, J., Price, N. D., … Wang, K. (2014). Systems approach to neurodegenerative disease biomarker discovery. *Annual Review of Pharmacology and Toxicology*, *54*, 457–481.

Lerner, R., Post, J. M., Ellis, S. R., Vos, D. R. N., Heeren, R. M. A., Lutz, B., & Bindila, L. (2018). Simultaneous lipidomic and transcriptomic profiling in mouse brain punches of acute epileptic seizure model compared to controls. *Journal of Lipid Research*, *59*, 283–297.

Liu, H., Chen, R., Wang, J., Chen, S., Xiong, C., Wang, J., … Mao, L. (2014). 1,5-Diaminonaphthalene hydrochloride assisted laser desorption/ionization mass spectrometry imaging of small molecules in tissues following focal cerebral ischemia. *Analytical Chemistry*, *86*, 10114–10121.

Llombart, V., Trejo, S. A., Bronsoms, S., Morancho, A., Feifei, M., Faura, J., … Montaner, J. (2017). Profiling and identification of new proteins involved in brain ischemia using MALDI-imaging-mass-spectrometry. *Journal of Proteomics*, *152*, 243–253.

Matsumoto, J., Nakanishi, H., Kunii, Y., Sugiura, Y., Yuki, D., Wada, A., … Yabe, H. (2017). Decreased 16:0/20:4-phosphatidylinositol level in the post-mortem prefrontal cortex of elderly patients with schizophrenia. *Scientific Reports*, *7*, 45050.

Matsumoto, J., Sugiura, Y., Yuki, D., Hayasaka, T., Goto-Inoue, N., Zaima, N., … Niwa, S. (2011). Abnormal phospholipids distribution in the prefrontal cortex from a patient with schizophrenia revealed by matrix-assisted laser desorption/ionization imaging mass spectrometry. *Analytical and Bioanalytical Chemistry*, *400*, 1933–1943.

McLean, J. A., Ridenour, W. B., & Caprioli, R. M. (2007). Profiling and imaging of tissues by imaging ion mobility-mass spectrometry. *Journal of Mass Spectrometry*, *42*, 1099–1105.

Meriaux, C., Franck, J., Wisztorski, M., Salzet, M., & Fournier, I. (2010). Liquid ionic matrixes for MALDI mass spectrometry imaging of lipids. *Journal of Proteomics*, *73*, 1204–1218.

Miyawaki, S., Imai, H., Hayasaka, T., Masaki, N., Ono, H., Ochi, T., … Saito, N. (2016). Imaging mass spectrometry detects dynamic changes of phosphatidylcholine in rat hippocampal CA1 after transient global ischemia. *Neuroscience*, *322*, 66–77.

Morosi, L., Giordano, S., Falcetta, F., Frapolli, R., Licandro, S. A., Matteo, C., … Davoli, E. (2017). Application of 3D mass spectrometry imaging to TKIs. *Clinical Pharmacology and Therapeutics*, *102*, 748–751.

Muller, L., Baldwin, K., Barbacci, D. C., Jackson, S. N., Roux, A., Balaban, C. D., … Woods, A. S. (2017). Laser desorption/ionization mass spectrometric imaging of endogenous lipids from rat brain tissue implanted with silver nanoparticles. *Journal of the American Society for Mass Spectrometry*, *28*, 1716–1728.

Nielsen, M. M., Lambertsen, K. L., Clausen, B. H., Meyer, M., Bhandari, D. R., Larsen, S. T., … Hansen, H. S. (2016). Mass spectrometry imaging of biomarker lipids for phagocytosis and signalling during focal cerebral ischaemia. *Scientific Reports*, *6*, 39571.

Park, K. M., Moon, J. H., Kim, K. P., Lee, S. H., & Kim, M. S. (2014). Relative quantification in imaging of a peptide on a mouse brain tissue by matrix-assisted laser desorption ionization. *Analytical Chemistry*, *86*, 5131–5135.

Powers, T. W., Holst, S., Wuhrer, M., Mehta, A. S., & Drake, R. R. (2015). Two-dimensional N-glycan distribution mapping of hepatocellular carcinoma tissues by MALDI-imaging mass spectrometry. *Biomolecules*, *5*, 2554–2572.

Powers, T. W., Jones, E. E., Betesh, L. R., Romano, P. R., Gao, P., Copland, J. A., … Drake, R. R. (2013). Matrix assisted laser desorption ionization imaging mass spectrometry workflow for spatial profiling analysis of N-linked glycan expression in tissues. *Analytical Chemistry*, *85*, 9799–9806.

Powers, T. W., Neely, B. A., Shao, Y., Tang, H., Troyer, D. A., Mehta, A. S., … Drake, R. R. (2014). MALDI imaging mass spectrometry profiling of N-glycans in formalin-fixed paraffin embedded clinical tissue blocks and tissue microarrays. *PLoS One*, *9*, e106255.

Prentice, B. M., Ryan, D. J., Van de, P. R., Caprioli, R. M., & Spraggins, J. M. (2018). Enhanced ion transmission efficiency up to m/ z 24000 for MALDI protein imaging mass spectrometry. *Analytical Chemistry*, *90*, 5090–5099.

Rabe, J. H., Sammour, A., Schulz, S., Munteanu, B., Ott, M., Ochs, K., … Hopf, C. (2018). Fourier transform infrared microscopy enables guidance of automated mass spectrometry imaging to predefined tissue morphologies. *Scientific Reports*, *8*, 313.

Ridenour, W. B., Kliman, M., McLean, J. A., & Caprioli, R. M. (2010). Structural characterization of phospholipids and peptides directly from tissue sections by MALDI traveling-wave ion mobility-mass spectrometry. *Analytical Chemistry*, *82*, 1881–1889.

Roux, A., Muller, L., Jackson, S. N., Post, J., Baldwin, K., Hoffer, B., … Woods, A. S. (2016). Mass spectrometry imaging of rat brain lipid profile changes over time following traumatic brain injury. *Journal of Neuroscience Methods*, *272*, 19–32.

Ruhaak, L. R., Xu, G., Li, Q., Goonatilleke, E., & Lebrilla, C. B. (2018). Mass spectrometry approaches to Glycomic and Glycoproteomic analyses. *Chemical Reviews*, *118*, 7886–7930.

Sans, M., Feider, C. L., & Eberlin, L. S. (2018). Advances in mass spectrometry imaging coupled to ion mobility spectrometry for enhanced imaging of biological tissues. *Current Opinion in Chemical Biology*, *42*, 138–146.

Seeley, E. H., & Caprioli, R. M. (2012). 3D imaging by mass spectrometry: A new frontier. *Analytical Chemistry*, *84*, 2105–2110.

Shanta, S. R., Kim, T. Y., Hong, J. H., Lee, J. H., Shin, C. Y., Kim, K. H., … Kim, K. P. (2012). A new combination MALDI matrix for small molecule analysis: Application to imaging mass spectrometry for drugs and metabolites. *Analyst*, *137*, 5757–5762.

Shanta, S. R., Zhou, L. H., Park, Y. S., Kim, Y. H., Kim, Y., & Kim, K. P. (2011). Binary matrix for MALDI imaging mass spectrometry of phospholipids in both ion modes. *Analytical Chemistry*, *83*, 1252–1259.

Shariatgorji, M., Nilsson, A., Goodwin, R. J., Svenningsson, P., Schintu, N., Banka, Z., … Andren, P. E. (2012). Deuterated matrix-assisted laser desorption ionization matrix uncovers masked mass spectrometry imaging signals of small molecules. *Analytical Chemistry*, *84*, 7152–7157.

Smith, J. C., Hou, W., Whitehead, S. N., Ethier, M., Bennett, S. A., & Figeys, D. (2008). Identification of lysophosphatidylcholine (LPC) and platelet activating factor (PAF) from PC12 cells and mouse cortex using liquid chromatography/multi-stage mass spectrometry (LC/MS3). *Rapid Communications in Mass Spectrometry*, *22*, 3579–3587.

Sparvero, L. J., Amoscato, A. A., Fink, A. B., Anthonymuthu, T., New, L. A., Kochanek, P. M., … Bayir, H. (2016). Imaging mass spectrometry

reveals loss of polyunsaturated cardiolipins in the cortical contusion, hippocampus, and thalamus after traumatic brain injury. *Journal of Neurochemistry*, *139*, 659–675.

Sparvero, L. J., Amoscato, A. A., Kochanek, P. M., Pitt, B. R., Kagan, V. E., & Bayir, H. (2010). Mass-spectrometry based oxidative lipidomics and lipid imaging: Applications in traumatic brain injury. *Journal of Neurochemistry*, *115*, 1322–1336.

Stauber, J., MacAleese, L., Franck, J., Claude, E., Snel, M., Kaletas, B. K., … Heeren, R. M. (2010). On-tissue protein identification and imaging by MALDI-ion mobility mass spectrometry. *Journal of the American Society for Mass Spectrometry*, *21*, 338–347.

Sugiura, Y., Konishi, Y., Zaima, N., Kajihara, S., Nakanishi, H., Taguchi, R., & Setou, M. (2009). Visualization of the cell-selective distribution of PUFA-containing phosphatidylcholines in mouse brain by imaging mass spectrometry. *Journal of Lipid Research*, *50*, 1776–1788.

Sugiura, Y., Shimma, S., Konishi, Y., Yamada, M. K., & Setou, M. (2008). Imaging mass spectrometry technology and application on ganglioside study; visualization of age-dependent accumulation of C20-ganglioside molecular species in the mouse hippocampus. *PLoS One*, *3*, e3232.

Takats, Z., Wiseman, J. M., Gologan, B., & Cooks, R. G. (2004). Mass spectrometry sampling under ambient conditions with desorption electrospray ionization. *Science*, *306*, 471–473.

Thiele, H., Heldmann, S., Trede, D., Strehlow, J., Wirtz, S., Dreher, W., … Maass, P. (2014). 2D and 3D MALDI-imaging: Conceptual strategies for visualization and data mining. *Biochimica et Biophysica Acta*, *1844*, 117–137.

Toghi, E. S., Yang, S., Wang, X., Shah, P., Li, X., & Zhang, H. (2014). Imaging of N-linked glycans from formalin-fixed paraffin-embedded tissue sections using MALDI mass spectrometry. *ACS Chemical Biology*, *9*, 2149–2156.

Trim, P. J., & Snel, M. F. (2016). Small molecule MALDI MS imaging: Current technologies and future challenges. *Methods*, *104*, 127–141.

Tyers, M., & Mann, M. (2003). From genomics to proteomics. *Nature*, *422*, 193–197.

Ucal, Y., Durer, Z. A., Atak, H., Kadioglu, E., Sahin, B., Coskun, A., … Ozpinar, A. (2017). Clinical applications of MALDI imaging technologies in cancer and neurodegenerative diseases. *Biochimica et Biophysica Acta*, *1865*, 795–816.

Varki, A. (2017). Biological roles of glycans. *Glycobiology*, *27*, 3–49.

Verhaert, P. D., Pinkse, M. W., Strupat, K., & Conaway, M. C. (2010). Imaging of similar mass neuropeptides in neuronal tissue by enhanced resolution MALDI MS with an ion trap - Orbitrap hybrid instrument. *Methods in Molecular Biology*, *656*, 433–449.

Villacrez, M., Hellman, K., Ono, T., Sugihara, Y., Rezeli, M., Ek, F., … Olsson, R. (2018). Evaluation of drug exposure and metabolism in locust and Zebrafish brains using mass spectrometry imaging. *ACS Chemical Neuroscience*, *9*, 1994–2000.

Wang, J., Wang, C., & Han, X. (2018). Enhanced coverage of lipid analysis and imaging by matrix-assisted laser desorption/ionization mass spectrometry via a strategy with an optimized mixture of matrices. *Analytica Chimica Acta*, *1000*, 155–162.

Wang, X., Han, J., Yang, J., Pan, J., & Borchers, C. H. (2015). Matrix coating assisted by an electric field (MCAEF) for enhanced tissue imaging by MALDI-MS. *Chemical Science*, *6*, 729–738.

Wang, Z., Cai, Y., Wang, Y., Zhou, X., Zhang, Y., & Lu, H. (2017). Improved MALDI imaging MS analysis of phospholipids using graphene oxide as new matrix. *Scientific Reports*, *7*, 44466.

Weishaupt, N., Caughlin, S., Yeung, K. K., & Whitehead, S. N. (2015). Differential anatomical expression of Ganglioside GM1 species containing d18:1 or d20:1 Sphingosine detected by MALDI imaging mass spectrometry in mature rat brain. *Frontiers in Neuroanatomy*, *9*, 155.

Whitehead, S. N., Chan, K. H., Gangaraju, S., Slinn, J., Li, J., & Hou, S. T. (2011). Imaging mass spectrometry detection of gangliosides species in the mouse brain following transient focal cerebral ischemia and long-term recovery. *PLoS One*, *6*, e20808.

Whitehead, S. N., Cheng, G., Hachinski, V., & Cechetto, D. F. (2005). Interaction between a rat model of cerebral ischemia and beta-amyloid toxicity: II. Effects of triflusal. *Stroke*, *36*, 1782–1789.

Whitehead, S. N., Gangaraju, S., Slinn, J., & Hou, S. T. (2010). Transient and bilateral increase in Neuropilin-1, Fer kinase and collapsin response mediator proteins within membrane rafts following unilateral occlusion of the middle cerebral artery in mouse. *Brain Research*, *1344*, 209–216.

Whitehead, S. N., Hachinski, V. C., & Cechetto, D. F. (2005). Interaction between a rat model of cerebral ischemia and beta-amyloid toxicity: Inflammatory responses. *Stroke*, *36*, 107–112.

Whitehead, S. N., Hou, W., Ethier, M., Smith, J. C., Bourgeois, A., Denis, R., … Figeys, D. (2007). Identification and quantitation of changes in the platelet activating factor family of glycerophospholipids over the course of neuronal differentiation by high-performance liquid chromatography electrospray ionization tandem mass spectrometry. *Analytical Chemistry*, *79*, 8539–8548.

Winter, M., Tholey, A., Kristen, A., & Rocken, C. (2017). MALDI mass spectrometry imaging: A novel tool for the identification and classification of amyloidosis. *Proteomics*, *17*, 1700236-1–1700236-9.

Woods, A. S., Colsch, B., Jackson, S. N., Post, J., Baldwin, K., Roux, A., … Balaban, C. (2013). Gangliosides and ceramides change in a mouse model of blast induced traumatic brain injury. *ACS Chemical Neuroscience*, *4*, 594–600.

Wu, C., Dill, A. L., Eberlin, L. S., Cooks, R. G., & Ifa, D. R. (2013). Mass spectrometry imaging under ambient conditions. *Mass Spectrometry Reviews*, *32*, 218–243.

Wu, Q., Comi, T. J., Li, B., Rubakhin, S. S., & Sweedler, J. V. (2016). On-tissue Derivatization via electrospray deposition for matrix-assisted laser desorption/ionization mass spectrometry imaging of endogenous fatty acids in rat brain tissues. *Analytical Chemistry*, *88*, 5988–5995.

Xiong, X., Xu, W., Eberlin, L. S., Wiseman, J. M., Fang, X., Jiang, Y., … Ouyang, Z. (2012). Data processing for 3D mass spectrometry imaging. *Journal of the American Society for Mass Spectrometry*, *23*, 1147–1156.

Yang, J., & Caprioli, R. M. (2011). Matrix sublimation/recrystallization for imaging proteins by mass spectrometry at high spatial resolution. *Analytical Chemistry*, *83*, 5728–5734.

Yang, J., & Caprioli, R. M. (2014). Matrix pre-coated targets for high throughput MALDI imaging of proteins. *Journal of Mass Spectrometry*, *49*, 417–422.

Ye, H., Mandal, R., Catherman, A., Thomas, P. M., Kelleher, N. L., Ikonomidou, C., & Li, L. (2014). Top-down proteomics with mass spectrometry imaging: A pilot study towards discovery of biomarkers for neurodevelopmental disorders. *PLoS One*, *9*, e92831.

Ye, H., Wang, J., Greer, T., Strupat, K., & Li, L. (2013). Visualizing neurotransmitters and metabolites in the central nervous system by high resolution and high accuracy mass spectrometric imaging. *ACS Chemical Neuroscience*, *4*, 1049–1056.

Zaima, N., Yoshioka, S., Sato, Y., Shinano, S., Ikeda, Y., & Moriyama, T. (2014). Enhanced specificity for phosphatidylcholine analysis by positive ion mode matrix-assisted laser desorption/ionization imaging mass spectrometry. *Rapid Communications in Mass Spectrometry*, *28*, 1453–1458.

Zavalin, A., Todd, E. M., Rawhouser, P. D., Yang, J., Norris, J. L., & Caprioli, R. M. (2012). Direct imaging of single cells and tissue at subcellular spatial resolution using transmission geometry MALDI MS. *Journal of Mass Spectrometry*, *47*, 1473–1481.

Zavalin, A., Yang, J., Haase, A., Holle, A., & Caprioli, R. (2014). Implementation of a Gaussian beam laser and aspheric optics for high spatial resolution MALDI imaging MS. *Journal of the American Society for Mass Spectrometry*, *25*, 1079–1082.

Zavalin, A., Yang, J., Hayden, K., Vestal, M., & Caprioli, R. M. (2015). Tissue protein imaging at 1 mum laser spot diameter for high spatial resolution and high imaging speed using transmission geometry MALDI TOF MS. *Analytical and Bioanalytical Chemistry*, *407*, 2337–2342.

Zhou, D., Guo, S., Zhang, M., Liu, Y., Chen, T., & Li, Z. (2017). Mass spectrometry imaging of small molecules in biological tissues using graphene oxide as a matrix. *Analytica Chimica Acta*, *962*, 52–59.

How to cite this article: Xu G, Li J. Recent advances in mass spectrometry imaging for multiomics application in neurology. *J Comp Neurol*. 2019;527:2158–2169. https://doi.org/10.1002/cne.24571